Available online at www.sciencedirect.com
ScienceDirect
Catalysis Today 122 (2007) 118–127
CATALYSIS TODAY
www.elsevier.com/locate/cattod

Selectivity of hydroxyl radical in the partial oxidation of aromatic compounds in heterogeneous photocatalysis

Giovanni Palmisano [a], Maurizio Addamo [a], Vincenzo Augugliaro [a], Tullio Caronna [b], Agatino Di Paola [a,*], Elisa García López [a], Vittorio Loddo [a], Giuseppe Marcì [a], Leonardo Palmisano [a], Mario Schiavello [a]

[a] *Dipartimento di Ingegneria Chimica dei Processi e dei Materiali, Facoltà di Ingegneria, Università degli Studi di Palermo, Viale delle Scienze, 90128 Palermo, Italy*

[b] *Dipartimento di Ingegneria Industriale, Facoltà di Ingegneria, Università degli Studi di Bergamo, Via Marconi 5, 24044 Dalmine (Bergamo), Italy*

Available online 31 January 2007

Abstract

The photocatalytic oxidation of different benzene derivatives has been investigated in order to understand how the substituent group affects the selectivity to hydroxylated compounds. Experimental runs were performed by using TiO_2 (Merck) aqueous suspensions at natural pH irradiated by near-UV light. The organic molecules used as substrate contained an electron withdrawing group (EWG) (nitrobenzene, cyanobenzene, benzoic acid, 1-phenylethanone), an electron donor one (EDG) (phenol, phenylamine, *N*-phenylacetamide) or both an EWG and an EDG (4-chlorophenol). The results clearly indicated that the primary photocatalytic oxidation of aromatic compounds containing an EDG gives rise mainly to *ortho* and *para* mono-hydroxy derivatives while in the presence of an EWG all the mono-hydroxy derivatives are obtained. This finding can open a new green route for the synthesis of hydroxylated aromatic compounds. Moreover, in the presence of both an ED and an EW group, as in the case of 4-chlorophenol and hydroxy-cyanobenzenes, the attack of the hydroxyl radical takes place only in the positions activated by –OH. A competing reaction pathway to total oxidation was also observed from the starting of the irradiation; this pathway was more important for compounds containing an EWG. This evidence can be explained by considering the strong interaction of these molecules with the TiO_2 surface. In fact, adsorption in the dark, measured for all the compounds, resulted to be significant only for molecules having strongly EWG's.

Keywords: Heterogeneous photocatalysis; Titanium dioxide; Selectivity of hydroxyl radical; Aromatic compounds

1. Introduction

Heterogeneous photocatalysis by using polycrystalline semiconductor oxides is an unconventional technology that has been mainly applied to degrade organic and inorganic pollutants both in vapour and liquid phases [1–3]. Its main advantages consist not only in the mild conditions under which the process is carried out, but also in the possibility to abate refractory, very toxic and non biodegradable molecules. Many semiconductor materials have been tested as photocatalysts but it is generally accepted that TiO_2, due to its low cost and high activity and stability under irradiation, is the most reliable material [2].

Applications of photocatalysis as a synthetic route have also been tested but they are not very common because photocatalytic reactions have always been considered as highly unselective processes [1–3]. Nevertheless synthesis of methanol from methane [4,5], conversion of carbon dioxide to useful chemicals [6,7] and production of hydrogen from water [7,8] have attracted attention, due to the prominent growth of chemical and energetic unconventional routes. Recently, some organic syntheses have been carried out by means of semiconductor oxides and visible light [9,10].

The studies on the photocatalytic oxidation of aromatic compounds have investigated the interactions of these species with the catalyst surface, the mechanism of photoreaction and the reaction kinetics [11–24]. The affinity of the aromatic substrates with the TiO_2 surface determines the occurrence of adsorption and photoadsorption in a more or less extent. Clearly, only the former can be measured with accuracy

* Corresponding author. Tel.: +39 091 6567229; fax: +39 091 6567280.
E-mail address: dipaola@dicpm.unipa.it (A. Di Paola).

0920-5861/$ – see front matter
doi:10.1016/j.cattod.2007.01.026

because, when irradiation starts, it is hard to discern the photoadsorption from the photoreactivity events. Many articles report data about adsorption of organic substrates in the dark [12–20]. Generally, the adsorption of aromatic species in the dark decreases by increasing the pH [12]. This result is explained by taking into account the presence of OH^- ions adsorbed onto the TiO_2 surface or localized in the liquid/solid interface (at basic pH's), that hampers the adsorption of hydroxylated aromatic intermediates existing mainly as anionic species. Conversely, Rao et al. [14] reported that the adsorption of 2-chlorophenol in the dark increases by increasing pH.

The significant adsorption of nitrobenzene [16] onto TiO_2 is affected by the presence of anions (Cl^-, HCO_3^-, SO_4^{2-}, NO_3^-) and by pH variations, the highest value being at pH of ca. 7. An FT-IR investigation on toluene and benzaldehyde adsorption [17] revealed that the former had a weak interaction with the TiO_2 surface for all of the used catalysts, while the latter exhibited different behaviours depending on the kind of TiO_2. Chan et al. [18] found a detectable adsorption of benzoic acid even if small quantities of TiO_2 were used.

In a study of the photocatalytic degradation of phenol and benzoic acid, Vione et al. [19] had an indirect evidence of considerably different interactions of these two species with the TiO_2 surface. The principal oxidation route of phenol degradation appeared to occur by means of OH radicals present in the solution bulk, while in the case of benzoic acid the main process took place on the photocatalyst surface by means of adsorbed OH radicals. This finding suggests that the interaction of benzoic acid with the TiO_2 surface is stronger than that of phenol, although it should be considered that the used TiO_2 was modified on its surface and this could have influenced the adsorption phenomena.

From the determination of intermediate compounds generated during the first oxidation steps, the mechanistic studies have stated that OH radicals are the species involved in the oxidation processes carried out in the presence of O_2. In particular, phenol oxidation was studied in the presence of TiO_2 anatase [11,12] and it was found that the main intermediates were hydroquinone, catechol and 1,2,4-trihydroxybenzene. In order to explain the formation of mono-hydroxy derivatives substituted only in *ortho* (catechol) and *para* (hydroquinone) positions, Peiró et al. [12] assumed that the phenol molecule reacted with an OH radical, forming an adduct that evolves giving rise to a phenoxy radical that is in resonance with radical structures in *ortho*- and *para*-positions. These resonance structures give rise to the two different mono-hydroxy derivatives and to other more complex intermediates, deriving from the reaction between two phenoxy radicals.

The mechanistic studies have been usually performed by investigating the degradation of only one aromatic compound so that no attempts were allowed to determine if the production of hydroxylated intermediates depended or not on the nature of the substituent group in the aromatic ring. Parra et al. [13] studied the kinetics of the photocatalytic oxidation of several substituted phenols and found that the highest and the lowest initial degradation rates, r_0, were those of 4-methoxyphenol and 4-nitrophenol, respectively. Hence, the electronic nature of the substituents can strongly influence the photoreactivity of phenolic compounds. Moreover the position of the $–NO_2$, –Cl and –COOH groups with respect to –OH did not influence significantly the r_0 values of the substrate, whereas the r_0 of the three di-hydroxylated benzenes were very different: $r_{0,meta} \gg r_{0,para} > r_{0,ortho}$. This behaviour was explained by taking into account the properties of –OH, which is a strongly electron donor and *ortho*-, *para*-orienting substituent. Another explanation of this feature was found in the keto-enol tautomeric equilibrium which could slow down the oxidation process: it is absent only in the case of the *meta*-isomer.

In this work, we report a study of the photocatalytic oxidation of several aromatic compounds in the presence of TiO_2, investigating the influence of the substituent group on the formation of mono-hydroxy derivatives. The organic molecules used as substrate were: nitrobenzene (NB), cyanobenzene (CB), benzoic acid (BA), 1-phenylethanone (1-PE), phenol (PH), phenylamine (PA), *N*-phenylacetamide (NPA), 4-chlorophenol (4-CP). The first four species contain an electron withdrawing group (EWG), the subsequent three an electron donor one (EDG) and the last one both an EW and an ED substituent. Aiming to reach a better understanding of the reactivity behaviour of mono-substituted aromatic species, the amounts of the previous compounds adsorbed onto the catalyst were also measured at equilibrium conditions. Moreover, the complete oxidation mechanism of CB was analysed in detail, as a case study, to better investigate the succeeding oxidation steps leading to the di-hydroxylation and eventually to the mineralization of this substrate.

2. Experimental

A gas seal Pyrex batch photoreactor of cylindrical shape, containing 0.5 l of aqueous suspension, was used for performing the reactivity experiments (see Fig. 1). The photoreactor was provided with ports in its upper section for the inlet and outlet of gases and for sampling. Moreover, for CB, the outlet gas was bubbled in a trap containing 250 ml of an aqueous solution of NaOH at pH 12 to fix the hydrogen cyanide escaping from the reacting system. A magnetic stirrer guaranteed a satisfactory suspension of the photocatalyst and the uniformity of the reacting mixture. A 125 W medium pressure Hg lamp (Helios Italquartz) was axially immersed within the photoreactor and it was cooled by water circulating through a Pyrex thimble; the temperature of the suspension was about 300 K. The radiation energy impinging on the suspension had an average value of 10 mW cm^{-2}; it was measured by using a radiometer UVX Digital, at $\lambda = 360$ nm.

For all of the runs, 0.4 g l^{-1} of TiO_2 Merck (100% anatase, BET surface area: ca. 10 m^2 g^{-1}) were used as the photocatalyst. The initial pH of the suspensions were the natural ones, ca. 4 for BA and ca. 6.5 for all the other compounds. The suspension was saturated by bubbling O_2 at atmospheric pressure for 1 h in the dark and then the lamp was turned on. The gas was continuously bubbled also during the runs that lasted 1.5 h.

Samples for analyses were withdrawn at fixed intervals of time; the catalyst was immediately separated from the aqueous

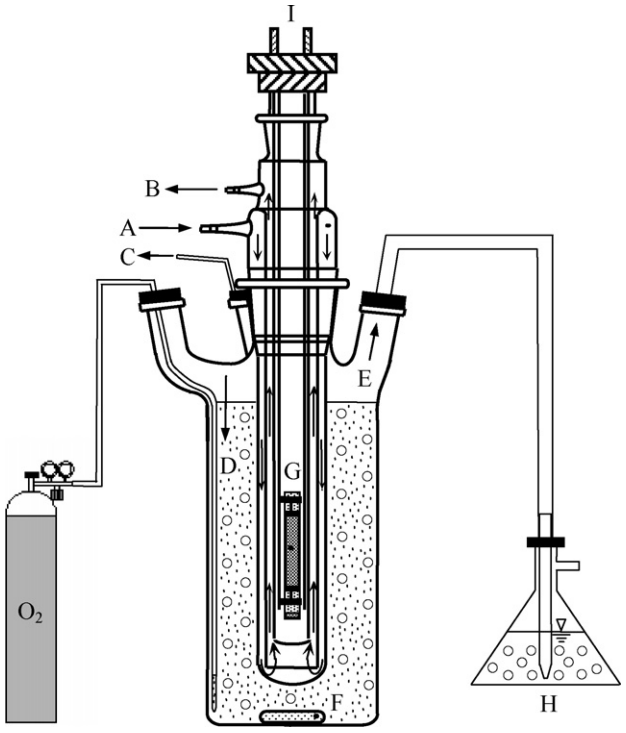

Fig. 1. Experimental set-up. (A and B) inlet and outlet of cooling water, (C) sampling port, (D) O_2 inlet, (E) gas exit, (F) magnetic bar, (G) lamp, (H) basic trap, and (I) lamp electric linkage.

solution by filtering through 0.45 μm Millex Millipore filters. For each sample a particular care was devoted to determine the concentrations of hydroxylation products (*ortho*, *meta* and *para*). The substrates and the intermediates produced during the reactions were analyzed with a HPLC Beckman Coulter (System Gold 126 Solvent Module and 168 Diode Array Detector), equipped with a Luna 5 μ Phenyl-Hexyl column (250 mm long × 2 mm i.d.). The HPLC eluent consisted of a 40 mM aqueous solution of KH_2PO_4, methanol and acetonitrile in different ratios depending on the substrate. The flow rate was 0.2 ml/min and the identification was carried out by comparison with authentical standard samples.

Total organic carbon (TOC) analyses were carried out by using a 5000A Shimadzu TOC analyser. These analyses allowed to determine the amount of organic carbon mineralized to CO_2 in the course of the reaction.

The quantitative determination of nitrate and formate ions was performed with a Dionex DX 120 ionic chromatograph, using a Dionex Ion Pac AS14 column (250 mm long × 4 mm i.d.). The eluent was an aqueous solution of $NaHCO_3$ (1 mM) and Na_2CO_3 (8 mM) at a flow rate of 1 ml/min. Cyanide and ammonium ions were determined by means of selective electrodes connected to an Orion 720A+ analyser. Cyanide was analysed by two electrodes: a reference one (Ion-Sensible Orion Model 90-01) and a selective one (Ion-Sensible Orion Model 94-06). An Ion-Sensible electrode (Orion, Model 95-01) was used for ammonium analyses.

All the used chemicals were purchased from Sigma–Aldrich.

3. Results

3.1. Adsorption and photocatalytic reactivity

Experiments of dark adsorption of the substrates on TiO_2 at room temperature were carried out for 1 h before starting the irradiation (initial substrate concentration ca. 0.5 mM). The substrate concentration measured before the addition of TiO_2 and after that the equilibrium was reached allowed to calculate the amount of adsorbed substrate. The figures obtained with the various compounds are reported in Table 1.

The photoreactivity results obtained with aromatic compounds containing an EWG or an EDG exhibited the same qualitative features. Figs. 2 and 3 show the results found with NB (EWG) and PA (EDG). These figures report the concentration values of the substrates and of their monohydroxylated products versus irradiation time. Fig. 4 shows the values of TOC measured during the irradiation of NB and PA.

It may be noted that the slope of the substrate disappearance plot extrapolated at zero time is quite higher than the sum of the slopes of the plots relative to the intermediates production. This feature derives from the fact that one of the main oxidation products, CO_2, arises from a further pathway in parallel with the previous ones. An experimental evidence of the occurrence of this parallel and kinetically very fast process derives from the

Table 1
Substituents, orientation, adsorption in the dark (after 1 h), conversions (after 1.5 h of irradiation), average overall yields in hydroxylated species and *o*:*m*:*p* ratios (determined during the first 45 min of irradiation) of the substrates studied

	Species						
	PH	PA	NPA	NB	CB	1-PE	BA
Group	–OH (EDG)	$–NH_2$ (EDG)	$–NHCOCH_3$ (slightly EDG)	$–NO_2$ (EWG)	–CN (EWG)	$–COCH_3$ (slightly EWG)	–COOH (EWG)
Orientation	*Ortho*, *para*	*Ortho*, *para*	*Ortho*, *para*	–	–	–	–
Adsorption in the dark (%)	Negligible	Negligible	Negligible	∼8	∼6	Negligible	Negligible
Conversion[a] (%)	∼70	∼40	∼50	∼50	∼60	∼55	∼40
Yield in OH^- derivatives (%)	∼75	∼50	∼60	∼20	∼30	∼30	∼25
o:*m*:*p* ratio[a]	54:1:45	50:0:50	20:3:77	29:34:37	45:30:25	39:21:40	43:29:28

Substrate initial concentration: ca. 0.5 mM.
[a] mol%.

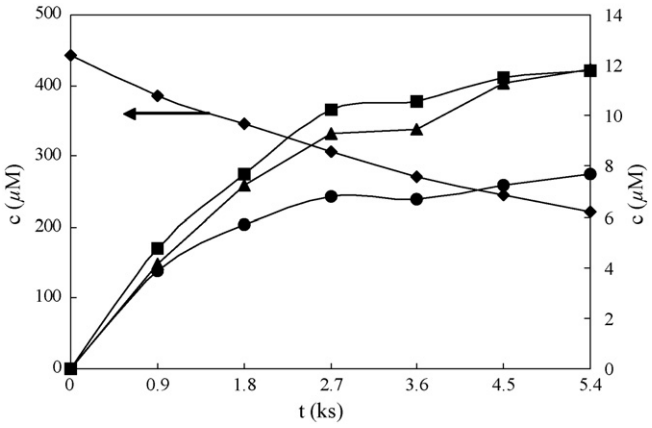

Fig. 2. Photocatalytic oxidation of nitrobenzene. (◆), nitrobenzene; (●), 2-hydroxy-nitrobenzene; (▲), 3-hydroxy-nitrobenzene; (■), 4-hydroxy-nitrobenzene. Substrate initial concentration: ca. 0.5 mM.

observation of the TOC results showing a decrease of the total organic carbon content, i.e. CO_2 production, from the starting of irradiation (see Fig. 4).

Table 1 reports the overall yield in mono-hydroxylated isomers obtained with each mono-substituted benzene compound. The conversions after 1.5 h of irradiation were in the 40–70 mol% range, being the lowest and the highest values those of PA (or BA) and PH, respectively. It may be noted that the conversion values were not influenced by the nature of the substituent.

The photoreactivity runs indicate that the aromatic molecules are oxidized in all cases and the concentrations of their oxidation products increase with irradiation time. When the photocatalytic reaction was carried out by using an aromatic compound containing an EDG, during the first 45 min of irradiation the mono-hydroxylated isomers were the main reaction products, with yields in the 50–75 mol% range. On the contrary, the yields in mono-hydroxylated isomers were in the 20–30 mol% range for the aromatic compounds containing an EWG.

Fig. 5 shows the reactivity results obtained by irradiation of 4-chlorophenol, a compound containing both an EW and an EG

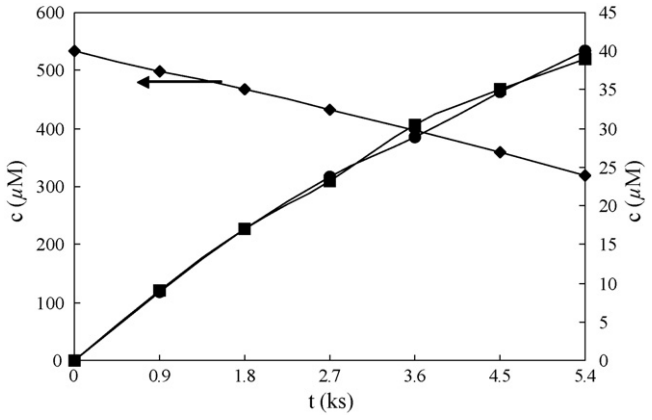

Fig. 3. Photocatalytic oxidation of phenylamine. (◆), phenylamine; (●), 2-hydroxy-phenylamine; (■), 4-hydroxy-phenylamine. Substrate initial concentration: ca. 0.5 mM.

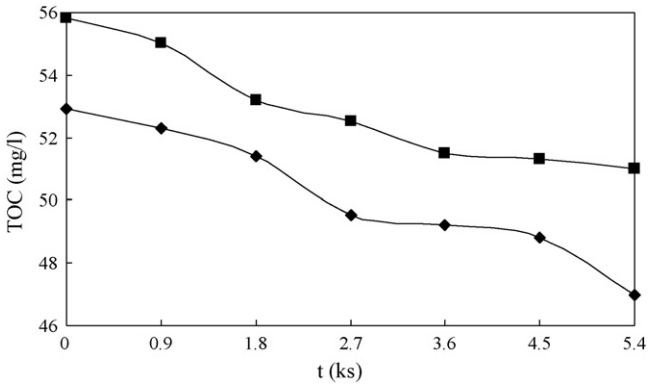

Fig. 4. TOC evolution during the photocatalytic oxidation of nitrobenzene (◆) and phenylamine (■). Substrate initial concentration: ca. 0.8 mM.

group. With this substrate the only obtained mono-hydroxy derivative was 4-chlorocatechol: i.e. OH radical enters only the activated position with respect to –OH. No traces of 4-chlororesorchinol were detected. The adsorption of 4-CP in the dark was negligible, its conversion after 1.5 h of irradiation was about 45% and the overall yield in 4-chlorocatechol was 26 mol%.

3.2. Cyanobenzene degradation

Fig. 6 shows the results obtained during the photocatalytic oxidation of cyanobenzene. During 1.5 h of irradiation the three mono-hydroxylated species and a di-hydroxylated species were identified. As shown in Table 1, CB, which reveals a significant adsorption in the dark, is mainly oxidized to CO_2. This process is responsible for the disappearance of the most part of the substrate as showed by Fig. 6 and by the TOC evolution in Fig. 7. The remaining CB molecules follow complex oxidation pathways according to which stable intermediate compounds are photoproduced and participate to adsorption–desorption phenomena between TiO_2 surface and aqueous solution. The primary intermediates of the CB degradation were 2-hydroxy-cyanobenzene (2-OH-CB), 3-hydroxy-cyanobenzene (3-OH-CB), and 4-hydroxy-cyanobenzene (4-OH-CB), along with

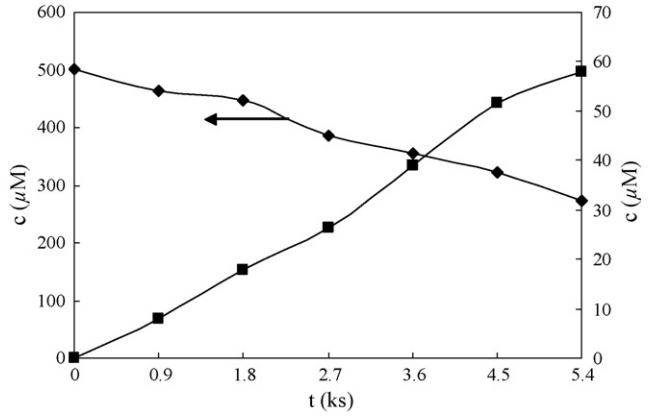

Fig. 5. Photocatalytic oxidation of 4-chlorophenol. (◆), 4-chlorophenol; (■), 4-chlorocatechol. Substrate initial concentration: ca. 0.5 mM.

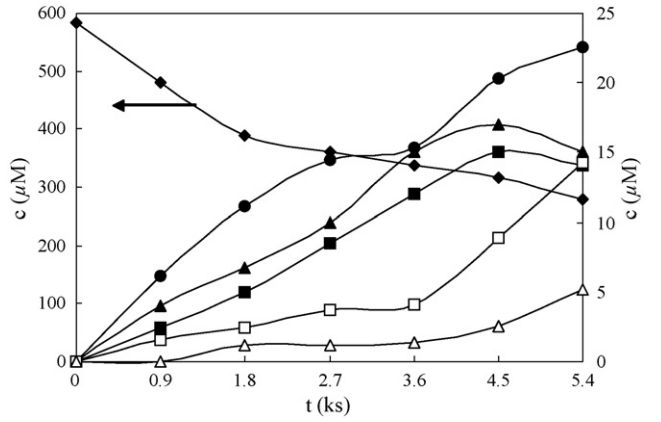

Fig. 6. Photocatalytic degradation of cyanobenzene. (◆), cyanobenzene; (●), 2-hydroxy-cyanobenzene; (▲), 3-hydroxy-cyanobenzene; (■), 4-hydroxy-cyanobenzene; (△), 3,4-dihydroxy-cyanobenzene; (□), cyanide. Substrate initial concentration: ca. 0.58 mM.

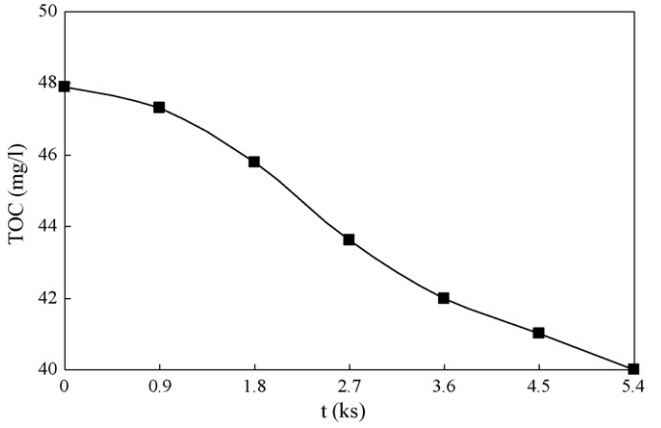

Fig. 7. TOC trend during the photocatalytic degradation of cyanobenzene. Substrate initial concentration: ca. 0.58 mM.

traces of phenol. Further identified intermediates were 3,4-dihydroxy-cyanobenzene (3,4-DOH-CB) and, among the open-ring intermediates, *trans*,*trans*-2,4-esandiendioic acid. The ionic species identified in the aqueous solution were CN^-, NH_4^+, NO_3^- and traces of $HCOO^-$.

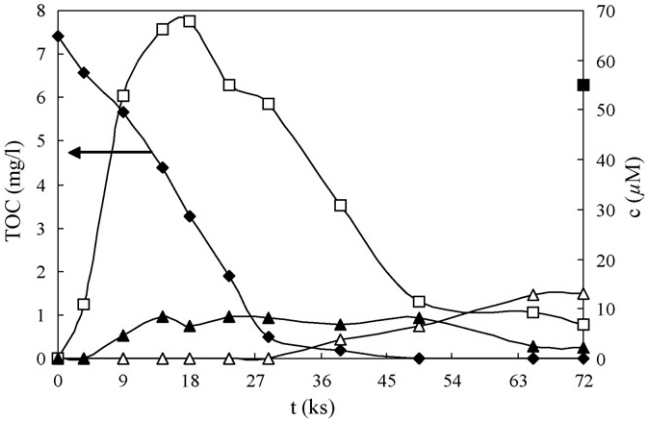

Fig. 8. Mineralization of cyanobenzene (initial concentration: 85 μM). (◆), TOC; (□), cyanide; (▲), ammonium; (△), nitrate; (■), cyanide found in the trap.

Table 2
Mass balance on nitrogen in the cyanobenzene mineralization run (duration of the run: ≈72 ks)

$c_{\text{cyanobenzene, initial}}$ (μM)	85
$c_{\text{cyanide, final}}$ (μM)	1.9
$c_{\text{ammonium, final}}$ (μM)	10.7
$c_{\text{cyanide in trap, final}}$ (μM)	32
$c_{\text{nitrate, final}}$ (μM)	37
$c_{\text{total nitrogen, final}}$ (μM)	81.6

The reported concentrations, *c*, are referred to the amount of nitrogen in each species.

From the observation of Fig. 6, it may be noted that the slopes at zero time of the lines interpolating the data of the mono-hydroxylated intermediates are different from zero while the slope of the line interpolating the concentration data of 3,4-DOH-CB is equal to zero. These features clearly indicate that the mono-hydroxylated species are produced through independent reactions in parallel involving the substrate while the di-hydroxylated species are produced by series reactions.

Fig. 8 shows the values of TOC and the concentrations of ammonium, nitrate and cyanide ions measured during 20 h of irradiation and the value of the cyanide concentration found in the basic trap at the end of the run. Table 2 reports the mass balance on nitrogen calculated for an experimental run during which no samples were withdrawn from the reaction ambient. In this case, the sum of nitrogen recovered as nitrate, ammonium, and cyanide ions amounted to ca. 96 mol% of the initial nitrogen concentration.

4. Discussion

4.1. Influence of the substituent group on the photocatalytic reactivity

The results of the photoreactivity runs carried out with the examined aromatic substrates have highlighted the occurrence from the starting of irradiation of at least two principal competing pathways: (i) photodegradation with production of CO_2 and (ii) formation of mono-hydroxylated species released into the bulk of the solution, in turn also transformed into di-hydroxylated compounds, open-ring species and eventually into CO_2.

The parallel oxidation route to complete mineralization was reported in literature for toluene [17] and nitrobenzene [16] and it should be stressed that it works at various extents from the starting of irradiation when the substrates have not a very high molecular weight, as in our case. It is obvious that the evolution to CO_2 is not a one-step process; it occurs through various oxidation steps involving unknown intermediate species whose main feature is that they are strongly adsorbed onto the irradiated TiO_2 surface without being released into the bulk of solution.

The data in Table 1 clearly indicate that the nature of the substituent strongly influences: (i) the adsorption of the aromatic substrate onto the surface of the catalyst and (ii) the position of the hydroxyl group entering the aromatic ring, giving rise to a regioselectivity in the mono-hydroxylated reaction products.

All the compounds containing an EDG revealed a negligible adsorption. Conversely a noticeable adsorption was observed in the presence of EW groups as $–NO_2$ and –CN. The negligible adsorption also found for 1-PE and BA could be explained by considering that their substituent groups have an electron withdrawing effect slighter than that of $–NO_2$ and –CN.

The above findings indicate that the presence of a certain additional electron density, induced in the aromatic ring by the presence of an EDG, is not beneficial for the molecule adsorption. On the contrary, the presence of a strongly EWG reduces the electron density of the aromatic ring, favouring the adsorption of the molecule onto the catalyst surface. This effect could support the reaction pathway leading to the production of CO_2 onto the TiO_2 surface and/or the oxidation of the substituent group with consequent lower yields in mono-hydroxylated species (see Table 1), as observed for the substrates containing an EWG.

Aromatic molecules can adsorb through the formation of Ti^{4+} (surface)··π electron or OH (surface)··π electron type complexes [25,26], and the latter one should be related to the production of mono-hydroxylated species under irradiation before their release in the solution bulk. For both kinds of adsorption, the more or less significant basic nature of the substituents, related to their withdrawing or donor capacity, could play a major role. All kinds of Lewis and Brönsted-Lowry acid–base sites are generally present at various extent on the surface of polycrystalline TiO_2, as revealed by FTIR spectroscopy [26,27], and consequently it is difficult to establish which sites are the most important for the adsorption in the dark.

As reported by Amalric et al. [28] the adsorption of organic compounds on the TiO_2 surface can be related to the K_{ow} coefficient, i.e. the octanol–water partition coefficient. The adsorption of aromatic molecules in the dark increases with K_{ow} [28]. The observed degradation rates k_{obs} of the mono substituted compounds studied in the present work well satisfy the correlation found among k_{obs} (expressed in ks^{-1}), K_{ow} and MR (molar refractivity) multiplied by a factor 1.1:

$$\log k_{obs} = 1.1(0.2 \log K_{ow} - 0.033\mathrm{MR} - 0.43) \quad (1)$$

where $\mathrm{MR} = [m(n^2 - 1)]/[d(n^2 + 2)]$ (Lorenz–Lorentz relationship).

All values of refractive index (n), molecular mass (m) and density (d) of the various compounds were found in literature [29]. The estimated and experimental values of k_{obs} are reported in Fig. 9.

The principal aspect, that must be stressed, concerns the selectivity of the OH radical attack to the aromatic ring in *ortho*-, *meta*- and *para*-positions; the attack seems to be strongly dependent on the kind of substituent (Table 1). It is worth noting that the yields and the *o:m:p* ratios reported in Table 1 were calculated from the concentrations measured in the first 45 min of irradiation. The assumption was made that during this time the reactivity of the mono-hydroxylated species is negligible. The yields data obtained starting from aromatic substrates containing an EDG indicate that the main mono-hydroxylated compounds were *ortho*- and *para*-isomers, while the *meta*-isomer was absent or it was present only in very small amounts. The behaviour exhibited when an EWG was present in the aromatic ring was completely different: no influence on the orientation of the mono-hydroxy substituent was observed, given that *ortho*-, *meta*-, and *para*-isomers were all present in significant amounts (>20%).

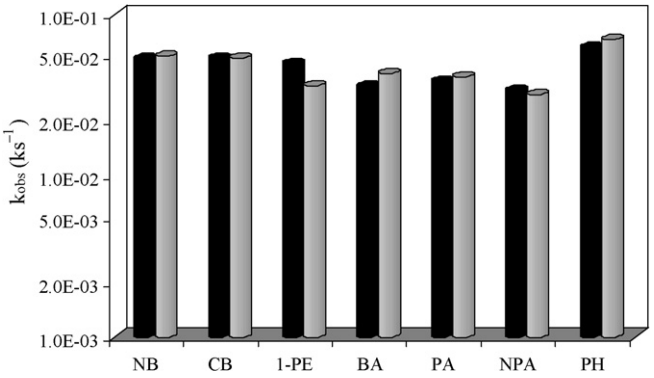

Fig. 9. Values of k_{obs} for the studied mono-substituted species: experimental data (black), data calculated from Eq. (1) (grey). Substrate initial concentration: ca. 0.5 mM.

The literature concerning the intermediates found during the photocatalytic oxidation of a large number of substituted aromatic compounds, using different kinds of TiO_2 under various experimental conditions [12–24], confirms this finding. Augugliaro et al. [22] reported the formation of 1-amino,2-hydroxy benzene and 1-amino,4-hydroxy benzene during the photocatalytic oxidation of phenylamine. Bhatkhande et al. [16] degraded nitrobenzene using TiO_2 and concentrated solar radiation. Since $–NO_2$ is an EWG they detected all the three mono-hydroxy derivatives as intermediates. Marcì et al. [17] studied the photodegradation of toluene on irradiated TiO_2 both in liquid and in gas phases. They found 4-methylphenol among the intermediates in liquid-solid regime. Chan et al. [18] realized a solar photocatalytic thin film cascade reactor for the treatment of benzoic acid and found the three mono-hydroxy derivatives as intermediates in similar concentrations.

It has been previously reported [14,15,24] that the presence of both an ED and an EW group gives rise to a behaviour similar to that observed when only an EDG is present. Rao et al. [14] studied the degradation of 2-chlorophenol and they found 2-chlorohydroquinone as one of the intermediates, i.e. the hydroxylation took place only in the *para*-position activated by the –OH group (see Scheme 1). They also identified catechol and 1,2,4-trihydroxy benzene indicating that the –OH group can replace –Cl. Guillard et al. [15] followed the degradation of 4-chlorophenol as a model reaction to investigate the properties of different industrial TiO_2 catalysts. They detected the intermediates showed in Scheme 2, which confirm that the hydroxylation takes place in the position activated by –OH, whose influence prevails on that of an EWG as –Cl, (halogens are *ortho*-, *para*-orienting). Similar results were found during the photocatalytic oxidation of *ortho*-, *meta*- and *para*-nitrophenols [24].

It is generally accepted that in heterogeneous photocatalysis the oxidation reactions occur through a mechanism involving OH radicals [1–3,30]. The reactivity of the hydroxyl radical has

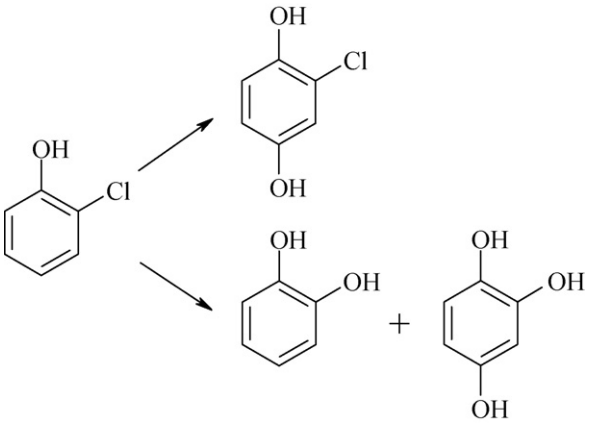

Scheme 1. Reaction mechanism of 2-chlorophenol photooxidation, catalyzed by TiO_2 in the presence of UV-light [14].

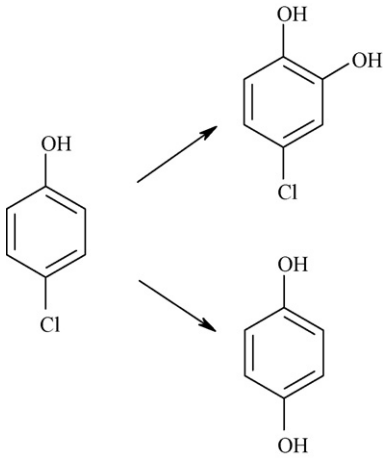

Scheme 2. Reaction mechanism of 4-chlorophenol photooxidation, catalyzed by TiO_2 in the presence of UV-light [15].

been the subject of intensive studies [31] and the correlation between the selectivity of the attack and the nature of the substituent in homogeneous reactions has been also recently studied with various experimental [19,32–35] and theoretical [36] methods. It is reported that the rate of addition of the OH radical to the aromatic rings is very high (the second order rate constant is ca. 10^9 to 10^{10} M^{-1} s^{-1}) and this could mean that the attack should be rather unselective. However, it is also reported that the ratio between the different regioisomers strongly depends on the oxidative power of the reaction medium [32–36]. The oxidation of the radical intermediates arising from the addition of a hydroxyl radical to the aromatic ring of the substrates of this work could occur in different ways: (i) by means of another hydroxyl radical for hydrogen abstraction; or (ii) by means of electron transfer followed by proton elimination. Consequently the further oxidation of the intermediates to the final products depends on the kind of substituent: an easier process would take place in the case of an EDG, with larger difficulty when the electron withdrawing ability of the group increases.

By taking into account also the position of the attack, the different intermediates will show different abilities to be

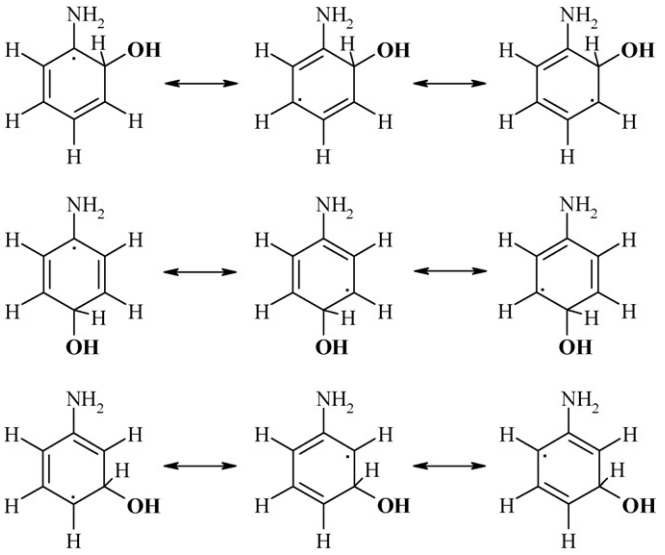

Scheme 3. Resonance structures of radical intermediates, produced during the oxidation of a compound containing an EDG.

oxidized. In fact, the behaviour of the aromatic compounds containing an EDG can be explained by the stabilization of the radical intermediates, whose resonance structures are showed in Scheme 3. In particular, the highest contribution to the stabilization is given by the formula with the unpaired electron on the carbon bonded to the EDG. This resonance structure can exist only when the hydroxyl radical enters *ortho*- and *para*-positions. On the contrary, a predominance of the *meta*-isomer would have been expected in the presence of an EWG, for which the above reported resonance structure is particularly unstable. Nevertheless this behaviour was not observed and all the three isomers were found: this could be explained hypothesising that the further oxidation process of the radical intermediate is in this case more difficult, especially considering that in the whole mechanism the presence of TiO_2 plays an important role.

On the basis of these results, it may be inferred that the heterogeneous photocatalytic oxidation of benzene derivatives is a selective reaction in the presence of an EDG: almost only the *ortho*- and *para*-isomers are formed, as summarized in

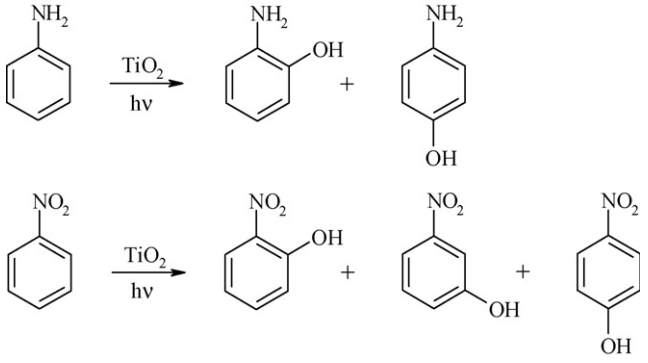

Scheme 4. Main hydroxylated products obtained during the photocatalytic oxidation of aromatic compounds containing either an electron donor or an electron-withdrawing group.

Scheme 4. Conversely all the three monohydroxy-derivatives are obtained when an EWG is present. It is worth noting that in the presence of both an ED and an EW group the monohydroxylation takes place only in free *ortho*- and *para*-positions with respect to the EDG.

4.2. Mechanism of cyanobenzene photocatalytic oxidation

In our experimental conditions, the partial oxidation of CB did not produce benzamide and benzoic acid that are the typical compounds obtained from the catalytic oxidation of CB. This feature indicates that the photocatalytic oxidation of CB follows a pathway completely different from the catalytic process. The presence of hydroxy-cyanobenzene isomers is a clear clue that the species responsible for CB partial oxidation are photoproduced OH radicals, which cause the breakage of C–H bonds. The OH radicals may also break the C–C bond between phenyl group and nitrilic one as indicated by the presence of cyanide ions in the reacting suspension from the starting of the photodegradation together with that of phenol, even if at very small concentration values.

The quick increase of the cyanide concentration observed after 1 h of irradiation (see Fig. 6) suggests that the breakage of the phenyl-nitrile bond is favoured when the aromatic ring is hydroxylated. As shown in Fig. 8, the cyanide concentration firstly increases, reaches a maximum value and therefore decreases. The decrease of cyanide ion concentration in the reacting dispersion is determined by two concomitant phenomena, i.e. the cyanide photocatalytic oxidation and the cyanide stripping from the solution caused by the bubbling oxygen. The free cyanide oxidation by photocatalysis is a well-known process [37–39] that has been investigated only at alkaline pHs: in these conditions CNO^- is produced and it is eventually photooxidized to NO_3^-. There is no information on the photocatalytic oxidation of free cyanide ions at neutral or acid pH's. In order to have qualitative indications on this process, a photoreactivity run was performed with a suspension containing only cyanide ions in the same experimental conditions used for CB but without bubbling oxygen during the irradiation. At the end of the run, cyanide ions partially disappeared, ammonium and nitrate ions were formed but no cyanate ions were detected. The absence of CNO^- ions may be determined by a hydrolysis reaction to NH_4^+ and CO_2 and/or a photocatalytic oxidation. It is worth noting that the complete hydrolysis of CNO^- (0.7 mM) in a solution at pH 6 in the absence of catalyst and light occurred in ca. 1 h. Even if it is not possible to exclude the occurrence of a photocatalytic transformation of the formed cyanate, the total absence of cyanate ions in the solution suggests that the main process is the fast hydrolysis reaction.

Scheme 5 reports the hypothesized reaction mechanism of CB mineralization. CO_2 can be obtained by fast oxidation of unknown adsorbed intermediates or through step-by-step formation of hydroxylated species, opening of the aromatic ring, and final oxidation of aliphatic compounds. Obviously, it cannot be excluded that the mono- and di-hydroxylated species can be subjected to a parallel mineralization pathway through adsorbed intermediates, similarly to what occurs with CB.

The second hydroxylation of the aromatic ring takes place with the formation of 3,4-dihydroxy-cyanobenzene (3,4-DOH-CB) which was identified by means of a commercial standard sample, and 2,3-dihydroxy-cyanobenzene (2,3-DOH-CB) and 2,5-dihydroxy-cyanobenzene (2,5-DOH-CB) whose identification cannot be firmly stated as the relative standards are not easily synthesizable. There are however strong clues supporting the above-proposed identification. In fact, three unknown peaks were observed in the chromatograms recorded during the CB oxidation. Two peaks are supposed to represent di-hydroxylated species, while the third peak is supposed to represent

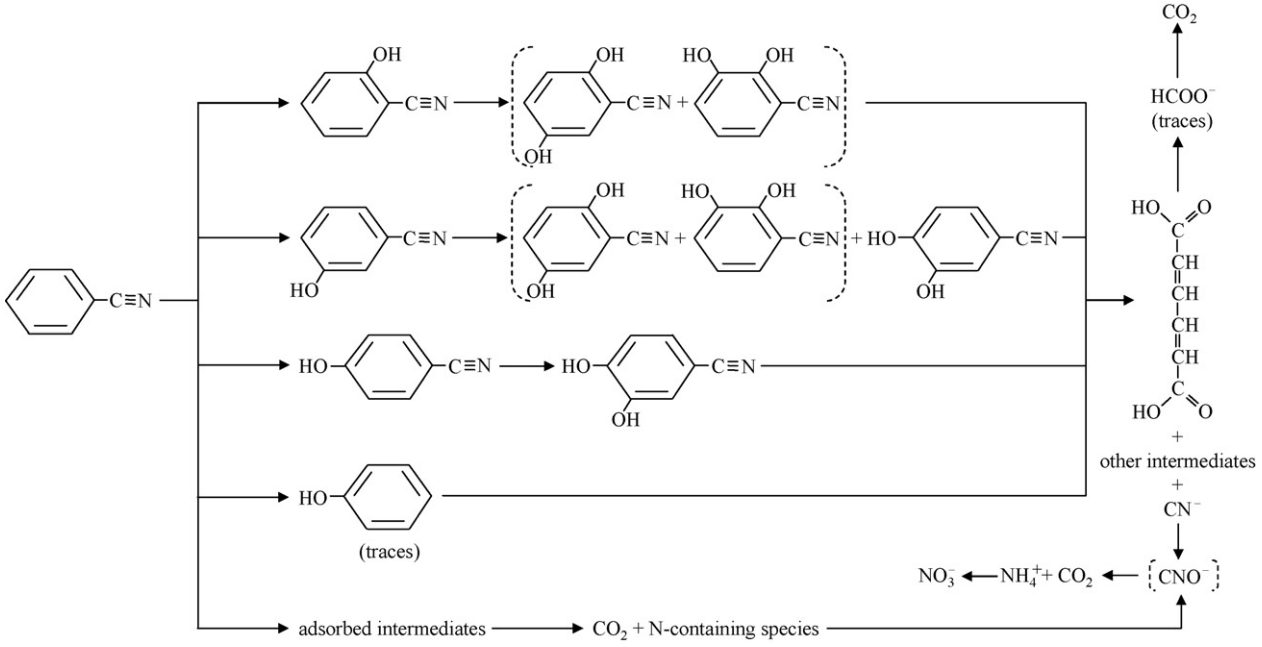

Scheme 5. Hypothesized mechanism of CB mineralization. The compounds in brackets were identified only indirectly.

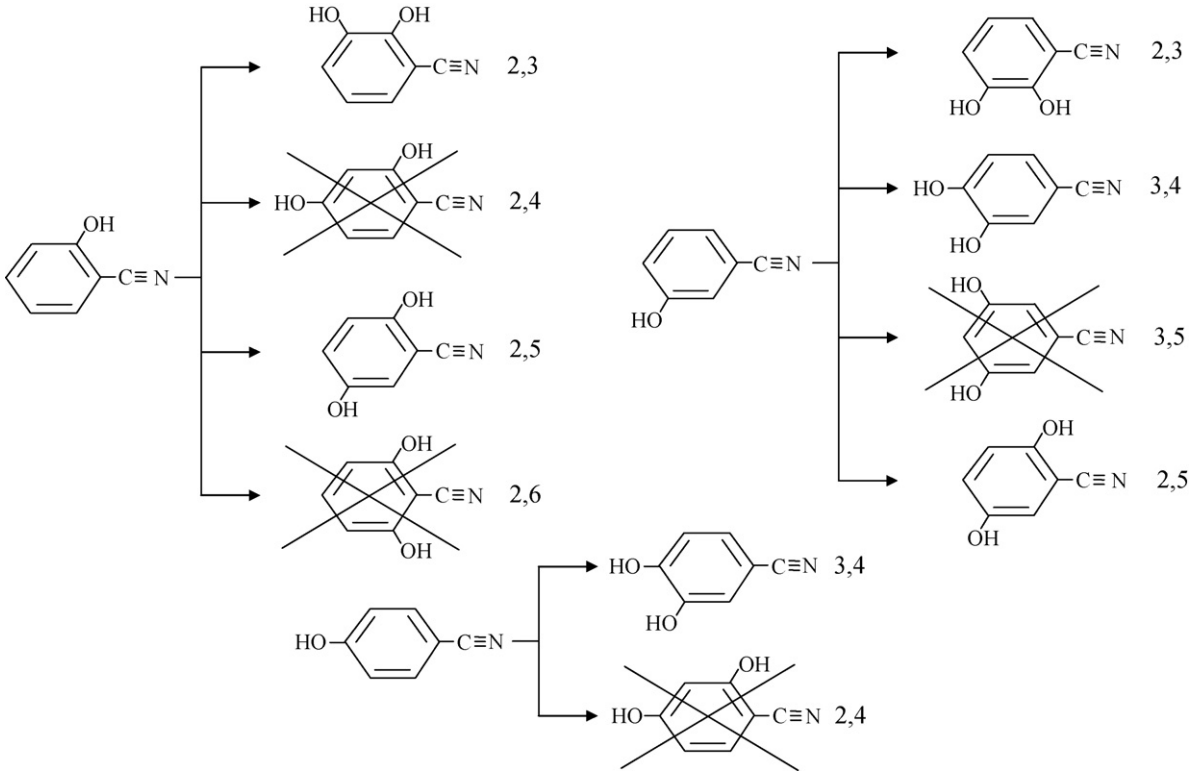

Scheme 6. Likely di-hydroxylated isomers derived from 2-hydroxy-cyanobenzene, 3-hydroxy-cyanobenzene and 4-hydroxy-cyanobenzene. The compounds not formed are crossed out.

either open-ring products or trihydroxylated species, since its retention time is very low.

The determination of the intermediates formed during the photocatalytic oxidation of standard 2-OH-CB, 3-OH-CB and 4-OH-CB solutions allowed to assign the first two peaks to 2,3-DOH-CB and 2,5-DOH-CB. In fact, both peaks appeared during the photodegradation of 2-OH-CB and 3-OH-CB but they were not detected during the photodegradation of 4-OH-CB that only produced the 3,4-DOH-CB species. As shown in Scheme 6, only the 2,3-DOH-CB and 2,5-DOH-CB are the di-hydroxylated isomers that can be obtained from both 2-OH-CB and 3-OH-CB. This last isomer gives rise also to 3,4-DOH-CB.

The chemical structure of the intermediate compounds detected in the reacting suspension indicates that the first attack of OH radicals takes place in all the three possible positions of the aromatic ring without any preference. On the contrary, the second attack appears to be selective in the –OH activated positions. This behaviour is similar to that reported for the photocatalytic oxidation of nitrobenzene and nitrophenols, in which $–NO_2$ (as –CN) is an EWG. In the case of nitrobenzene, indeed, all the three mono-hydroxylated isomers were found as photooxidation products [16] while with nitrophenols only the –OH activated isomers were detected [24].

5. Conclusions

Photocatalytic reactions can be used to obtain mono-hydroxylated aromatic derivatives in fairly to good yields. Under irradiation, the aromatic compounds photoadsorbed on the TiO_2 surface undergo two competing reaction pathways: (i) hydroxylation of the aromatic ring or (ii) multi-step oxidation reactions to complete mineralization.

In the case of compounds containing an electron donor group, the OH radical attack follows the expected selectivity rules, obtaining substitution in *ortho*- and *para*-positions of aromatic molecules. In the presence of an electron-withdrawing group, the attack is unselective, and a mixture of all the three possible isomers is obtained. The adsorption of the substrates onto the TiO_2 surface is a relevant factor to be considered in the formation of the mono-hydroxy derivatives.

Acknowledgement

The authors wish to thank MIUR (Rome) for financial support.

References

[1] M. Schiavello (Ed.), Photocatalysis and Environment. Trends and Applications, Kluwer, Dordrecht, 1988.
[2] A. Fujishima, K. Hashimoto, T. Watanabe, TiO_2 Photocatalysis. Fundamentals and Applications, BKC Inc., Tokyo, 1999.
[3] A. Fujishima, T.N. Rao, D.A. Tryk, J. Photochem. Photobiol. C: Photochem. Rev. 1 (2000) 1.
[4] Y. Hu, S. Higashimoto, S. Takahashi, Y. Nagai, M. Anpo, Catal. Lett. 100 (2005) 35.
[5] C.E. Taylor, Top. Catal. 32 (2005) 179.
[6] G.R. Dey, A.D. Belapurkar, K. Kishore, J. Photochem. Photobiol. A: Chem. 163 (2004) 503.
[7] S. Ichikawa, R. Doi, Catal. Today 27 (1996) 271.

[8] P. Maruthamuthu, M. Ashokkumar, Int. J. Hydr. En. 14 (1989) 275.
[9] T. Caronna, C. Gambarotti, L. Palmisano, C. Punta, F. Recupero, Chem. Commun. (2003) 2350.
[10] K.V. Subba Rao, B. Srinivas, M. Subrahmanyam, A.R. Prasad, Chem. Commun. (2000) 1533.
[11] I. Ilisz, A. Dombi, Appl. Catal. A: Gen. 180 (1999) 35.
[12] A.M. Peiró, J.A. Ayllón, J. Peral, X. Doménech, Appl. Catal. B: Environ. 30 (2001) 359.
[13] S. Parra, J. Olivero, L. Pacheco, C. Pulgarin, Appl. Catal. B: Environ. 43 (2003) 293.
[14] N.N. Rao, A.K. Dubey, S. Mohanty, P. Khare, R. Jain, S.N. Kaul, J. Hazard. Mat. B101 (2003) 301.
[15] C. Guillard, J. Disdier, J.-M. Herrmann, C. Lehaut, T. Chopin, S. Malato, J. Blanco, Catal. Today 54 (1999) 217.
[16] D.S. Bhatkhande, V.G. Pangarkar, A.A.C.M. Beenackers, Water Res. 37 (2003) 1223.
[17] G. Marcì, M. Addamo, V. Augugliaro, S. Coluccia, E. García-López, V. Loddo, G. Martra, L. Palmisano, M. Schiavello, J. Photochem. Photobiol. A: Chem. 160 (2003) 105.
[18] A.H.C. Chan, C.K. Chan, J.P. Barford, J.F. Porter, Water Res. 37 (2003) 1125.
[19] D. Vione, C. Minero, V. Maurino, M.E. Carlotti, T. Picatonotto, E. Pelizzetti, Appl. Catal. B: Environ. 58 (2005) 79.
[20] G. Palmisano, M. Addamo, V. Augugliaro, T. Caronna, E. García-López, V. Loddo, L. Palmisano, Chem. Commun. (2006) 1012.
[21] P. Piccinini, C. Minero, M. Vincenti, E. Pelizzetti, Catal. Today 39 (1997) 187.
[22] V. Augugliaro, A. Bianco Prevot, V. Loddo, G. Marcì, L. Palmisano, E. Pramauro, M. Schiavello, Res. Chem. Intermed. 26 (2000) 413.
[23] G. Mailhot, L. Hykrdová, J. Jirkovský, K. Lemr, G. Grabner, M. Bolte, Appl. Catal. B: Environ. 50 (2004) 25.
[24] A. Di Paola, V. Augugliaro, L. Palmisano, G. Pantaleo, E. Savinov, J. Photochem. Photobiol. A: Chem. 155 (2003) 207.
[25] M. Nagao, Y. Suda, Langmuir 5 (1989) 42.
[26] M. Primet, P. Pichat, M. Mathieu, J. Phys. Chem. 75 (1971) 1216.
[27] M. Primet, P. Pichat, M. Mathieu, J. Phys. Chem. 75 (1971) 1221.
[28] L. Amalric, C. Guillard, E. Blanc-Brude, P. Pichat, Water Res. 30 (1996) 1137, and references therein.
[29] http://chemfinder.cambridgesoft.com; http://esc.syrres.com/interkow/webprop.exe CAS = CASNUMBER.
[30] L. Linsebigler, G. Lu, J.T. Yates Jr., Chem. Rev. 95 (1995) 735, and references therein.
[31] C. Walling, Acc. Chem. Res. 8 (1975) 125.
[32] C. Walling, R.A. Johnson, J. Am. Chem. Soc. 97 (1975) 363.
[33] S. Ito, A. Mitarai, K. Hikino, M. Dirama, K. Sasaki, J. Org. Chem. 57 (1992) 6937.
[34] M.P. DeMatteo, J.S. Poole, X. Shi, R. Sachdeva, P.G. Hatcher, C.M. Hadad, M.S. Platz, J. Am. Chem. Soc. 127 (2005) 7094.
[35] G. Albarran, R.H. Schuler, J. Phys. Chem. A 109 (2005) 9363.
[36] A.B.J. Parusel, R. Schamschule, G. Kolher, Croat. Chem. Acta 73 (2000) 359, and references therein.
[37] S.N. Frank, A.J. Bard, J. Am. Chem. Soc. 99 (1977) 303.
[38] V. Augugliaro, V. Loddo, G. Marcì, L. Palmisano, M.J. López-Muñoz, J. Catal. 166 (1997) 272.
[39] V. Augugliaro, J. Blanco-Gálvez, J. Cáceres-Vázquez, E. García-López, V. Loddo, M.J. López-Muñoz, S. Malato-Rodríguez, G. Marcì, L. Palmisano, M. Schiavello, J. Soria Ruiz, Catal. Today 54 (1999) 245.